Visual Neuroscience (2000), **17**, 567–578. Printed in the USA.

Morphology of wide-field bistratified and diffuse human retinal ganglion cells

BETH B. PETERSON AND DENNIS M. DACEY

Department of Biological Structure, The University of Washington, Seattle

(RECEIVED December 2, 1999; ACCEPTED February 9, 2000)

Abstract

To study the detailed morphology of human retinal ganglion cells, we used intracellular injection of horseradish peroxidase and Neurobiotin to label over 1000 cells in an *in vitro*, wholemount preparation of the human retina. This study reports on the morphology of 119 wide-field bistratified and 42 diffuse ganglion cells. Cells were analyzed quantitatively on the basis of dendritic-field size, soma size, and the extent of dendritic branching. Bistratified cells were similar in dendritic-field diameter (mean ± S.D. = 682 ± 130 μm) and soma diameter (mean ± S.D. = 18 ± 3.3 μm) but showed a broad distribution in the extent of dendritic branching (mean ± S.D. branch point number = 67 ± 32; range = 15–167). Differences in the extent of branching and in dendritic morphology and the pattern of branching suggest that the human retina may contain at least three types of wide-field bistratified cells. Diffuse ganglion cells comprised a largely homogeneous group whose dendrites ramified throughout the inner plexiform layer. The diffuse cells had similar dendritic-field diameters (mean ± S.D. = 486 ± 113 μm), soma diameters (mean ± S.D. = 16 ± 2.3 μm), and branch points numbers (mean ± S.D. = 92 ± 32). The majority had densely branched dendritic trees and thin, very spiny dendrites with many short, fine, twig-like thorny processes. Five of the diffuse cells had much more sparsely branched dendritic trees (<50 branch points) and less spiny dendrites, suggesting that there are possibly two types of diffuse ganglion cells in human retina. Although the presence of a diversity of large bistratified and diffuse ganglion cells has been observed in a variety of mammalian retinas, little is known about the number of cell types, their physiological properties, or their central projections. Some of the human wide-field bistratified cells in the present study, however, show morphological similarities to monkey large bistratified cells that are known to project to the superior colliculus.

Keywords: Human retina, Ganglion cells, Bistratified, Diffuse

Introduction

Bistratified ganglion cells in mammalian retina project to the lateral geniculate nucleus (LGN) and midbrain targets, and are known to mediate such functions as color opponency and direction selectivity. In rabbit retina, the detailed morphology and physiology of ON–OFF direction-selective bistratified ganglion cells has been well described (Barlow et al., 1964; Oyster & Barlow, 1967; Amthor et al., 1984, 1989*a*; Famiglietti, 1992; Yang & Masland, 1992; Oyster et al., 1993; Vaney, 1994). In cat retina, while several types of bistratified ganglion cells have been morphologically and physiologically identified (O'Brien et al., 1999), none of the cells exhibited directional selectivity, and their function and central projections are not known. In primate retina, a diversity of bistratified ganglion cells has been described in Golgi studies of human retina (Kolb et al., 1992) and in retrograde labeling studies of macaque retina (Rodieck & Watanabe, 1993), yet only the small bistratified, or blue-ON color-opponent cell type has been well characterized (Dacey, 1993*a*; Dacey & Lee, 1994; Ghosh et al., 1996). Although no direction-selective ganglion cells have yet been identified in primate retina, Kolb et al. (1992), in their Golgi study of human retina, reported finding a bistratified ganglion cell that was morphologically similar to the ON–OFF direction-selective ganglion cells described in rabbit retina. In monkey retina, Rodieck and Watanabe (1993) described a diverse group of large bistratified cells that project to the superior colliculus; nothing is known about the physiological properties of these cells.

Diffuse ganglion cells have been observed in dog (Ramon y Cajal, 1892), cat (Pu et al., 1994; O'Brien et al., 1999), monkey (Polyak, 1941; Rodieck & Watanabe, 1993), chimpanzee (Polyak, 1941), and human (Kolb et al., 1992) retina. These studies suggest that there may be at least three types of diffuse ganglion cells in mammalian retina, yet there have been no quantitative studies of the morphology of diffuse cells and little is known of their physiological properties and central projections. As a first step toward characterizing both wide-field bistratified and diffuse ganglion cell types in human retina, we have quantitatively analyzed a large sample of 161 intracellularly stained ganglion cells based on dendritic-field size, soma size, and the extent of dendritic branching. Our findings suggest that the human retina may contain at

Address correspondence and reprint requests to: Dennis M. Dacey, Department of Biological Structure, Box 357420, The University of Washington, Seattle, WA 98195-7420, USA.

least three types of bistratified cells beyond the small bistratified cell, and possibly two types of diffuse ganglion cells. Morphological comparison of the wide-field bistratified cells of the present study with retrogradely labeled monkey ganglion cells suggests that some of the human wide-field bistratified cells may represent correlates of monkey large bistratified cells known to project to the superior colliculus.

Materials and methods

In vitro intracellular injection and histology

We have previously described the *in vitro* retinal whole-mount preparation and intracellular injection technique (Dacey & Petersen, 1992; Dacey, 1993*a*). Human eyes (n = 46, age range 16–82 years) were obtained 90–120 min after death from donors to the Lions Eye Bank at the University of Washington. Retinas were dissected free of the sclera and choroid in continuously oxygenated culture medium (Ames, Sigma Chemical Co., St. Louis, MO) and placed flat in a superfusion chamber on the stage of a light microscope. There was no apparent deterioration in the morphology of cells maintained in the chamber for ~8–10 h.

Ganglion cells were observed under episcopic illumination following *in vitro* staining with acridine orange. Intracellular injections were made into fluorescing cells with electrodes filled with Lucifer yellow (~2%; Aldrich Chemical, Milwaukee, WI) in 20 mM, pH 7.0 MOPS buffer (Sigma Chemical Co., St Louis, MO) and either rhodamine-conjugated horseradish peroxidase (HRP) (~4%; Sigma Chemical Co., St Louis, MO) or Neurobiotin (~4%; Vector Labs, Burlingame, CA). Lucifer yellow fluorescence in the electrode and acridine orange fluorescence of ganglion cells were observed with the same excitation filter (410–490 nm; barrier filter 515 nm), permitting direct observation of the electrode tip as it penetrated a cell. Successful penetration was confirmed by passing Lucifer yellow into an impaled cell. Ganglion cells were then filled with either rhodamine-conjugated HRP or Neurobiotin.

Following an experiment, retinas were fixed for 2–3 h in phosphate-buffered fixative (2% glutaraldehyde, 2% paraformaldehyde or 4% paraformaldehyde; 0.1 M, pH 7.4). Cells injected with rhodamine-conjugated HRP were revealed using diaminobenzidine (DAB) as the chromogen. Retinas were incubated in the DAB solution (0.1% in 0.1 M phosphate buffer, pH 7.4) for 5 min, then H_2O_2 (0.003%) was added and the retinas further incubated for 3–4 min. Retinas were rinsed in buffer, whole mounted on gelatin coated slides, air dried, then dehydrated in a graded alcohol series, cleared in xylene, and coverslipped.

Neurobiotin-injected cells were revealed by HRP histochemistry using the Vector ABC protocol (Vector, Elite kit). Retinas fixed in 4% paraformaldehyde were placed in 0.5% TritonX 100 (0.1 M phosphate buffer, pH 7.4) for 3 h at room temperature, then incubated in buffer containing the Vector avidin-biotin-HRP complex for 3 h. The retinas were rinsed in buffer for 1 h and processed for HRP histochemistry using DAB as the chromogen as described above.

Data analysis

The location of every injected ganglion cell relative to the foveal center was recorded for each retina. A camera-lucida tracing of the dendritic tree (total magnification, 480×) and an outline of the cell body (total magnification, 1940×) were made for each cell. Dendritic-field area was determined by tracing a convex polygon around the perimeter of the traced dendritic tree and entering the outline into a computer *via* a graphics tablet. Dendritic-field diameter was expressed as the diameter of a circle with the same area as that of the polygon. Similarly, cell body size was expressed in terms of an equivalent diameter.

The extent of dendritic branching was quantified as "number of branch points" by counting the terminal tips of the dendritic branches of the cells in the camera-lucida tracings. Total dendritic branch points were counted for each cell independently by two observers. For cells exhibiting many fine dendritic spines and twig-like branchlets, only processes greater than 10 μm in length were counted as branches. This was based on our observation that for ganglion cells where dendritic branches can be unambiguously distinguished from dendritic spines, the longest spines measured were 6–7 μm in length.

Dendritic stratification in the inner plexiform layer (IPL) was determined by taking measurements with reference to the ganglion cell layer/IPL border and the inner nuclear layer/IPL border at multiple locations in the dendritic tree. In our preparation, shrinkage in the plane of the retina was minimal (~2%), but we estimate about a 60–70% vertical shrinkage as a result of tissue processing. At the eccentricities of the cells in the present study, the thickness of the IPL ranged from about 9 μm near the mid periphery to about 4 μm in the far periphery. While it was possible to determine if a process ramified in the inner or outer half of the IPL, it was not possible to measure with reasonable accuracy the exact depth of stratification with the 1-μm scale of the microscope's fine focus knob.

Results

Cell identification

This study includes a sample of 119 wide-field bistratified and 42 diffuse ganglion cells derived from a larger sample of over 1000 intracellularly filled human ganglion cells representing a diversity of morphological cell types (Dacey et al., 1991). Cells classified as bistratified had dendrites that formed two arbors discretely stratified in both the inner and outer portions of the IPL. The wide-field bistratified ganglion cells of the present study were distinguished from the previously described small bistratified ganglion cell type (Dacey, 1993*a*) by the size of the dendritic field. This distinction can be seen in Fig. 1, where the dendritic-field diameters of wide-field bistratified and small bistratified ganglion cells are plotted as a function of eccentricity. Cells classified as wide-field bistratified formed a cluster distinct from the small bistratified cell type.

The 42 ganglion cells classified as diffuse had dendritic arbors that appeared to course throughout the IPL. The dendritic fields of these cells were also quite large but were in general somewhat smaller than the wide-field bistratified cells (Fig. 2). The dendritic morphology of diffuse ganglion cells was also distinct from the wide-field bistratified cells, as described below.

Wide-field bistratified ganglion cells

The wide-field bistratified ganglion cells were all similar in dendritic-field size. They form a single cluster in the scatter plot of Fig. 3a, where dendritic-field diameter (mean ± S.D. = 682 ± 130 μm) has been plotted as a function of eccentricity. The cells were also similar in that they had medium size somas (mean ± S.D. = 18 ± 3.3 μm), as illustrated in the plot of Fig. 3b. When the total number

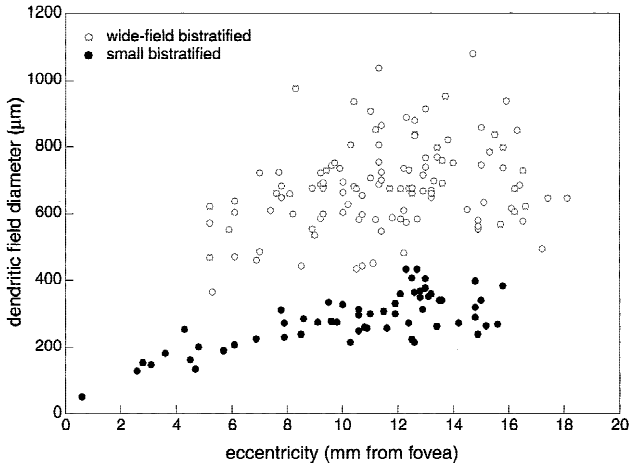

Fig. 1. Wide-field bistratified ganglion cells formed a cluster distinct from the small bistratified cell when plotted for dendritic-field diameter as a function of eccentricity. Data for small bistratified cells was taken from a previous study (Dacey, 1993*a*).

of branch points was plotted as a function of eccentricity, however, the cells showed a broad distribution, with a mean ± S.D. branch point number of 67 ± 32 and a range of 15–167 (Fig. 3c). Despite this diversity in the extent of dendritic branching, no clustering based on branch point number was observed (Fig. 3c).

Along with a diversity in the number of dendritic branch points, the wide-field bistratified cells also differed in their dendritic morphology and pattern of branching. This is illustrated in Fig. 4 with camera-lucida tracings of three cells representative of the group as a whole. About 30% of the bistratified cells had rather thick, smooth or slightly spiny dendrites and a simple, radiate pattern of branching (Fig. 4a). All of these cells had sparsely branched dendritic trees and some of them superficially resembled the previously described human large sparse monostratified cells (Peterson & Dacey, 1999) in the small number of overlapping dendrites. The

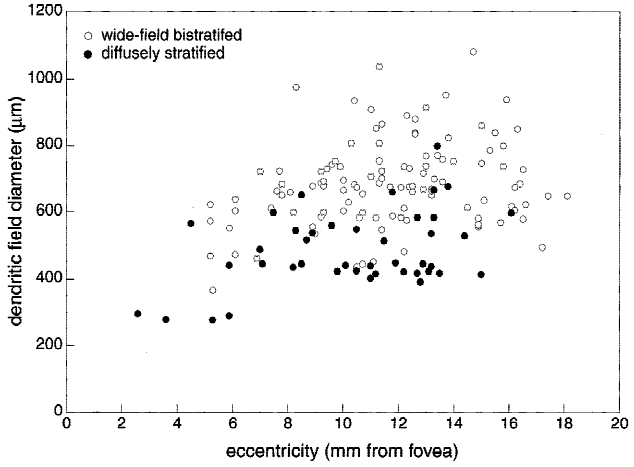

Fig. 2. Wide-field bistratified and diffuse ganglion cells plotted by dendritic-field diameter *vs.* eccentricity. All cells had large dendritic fields though the bistratified cells on the whole were somewhat larger than the diffuse ganglion cells.

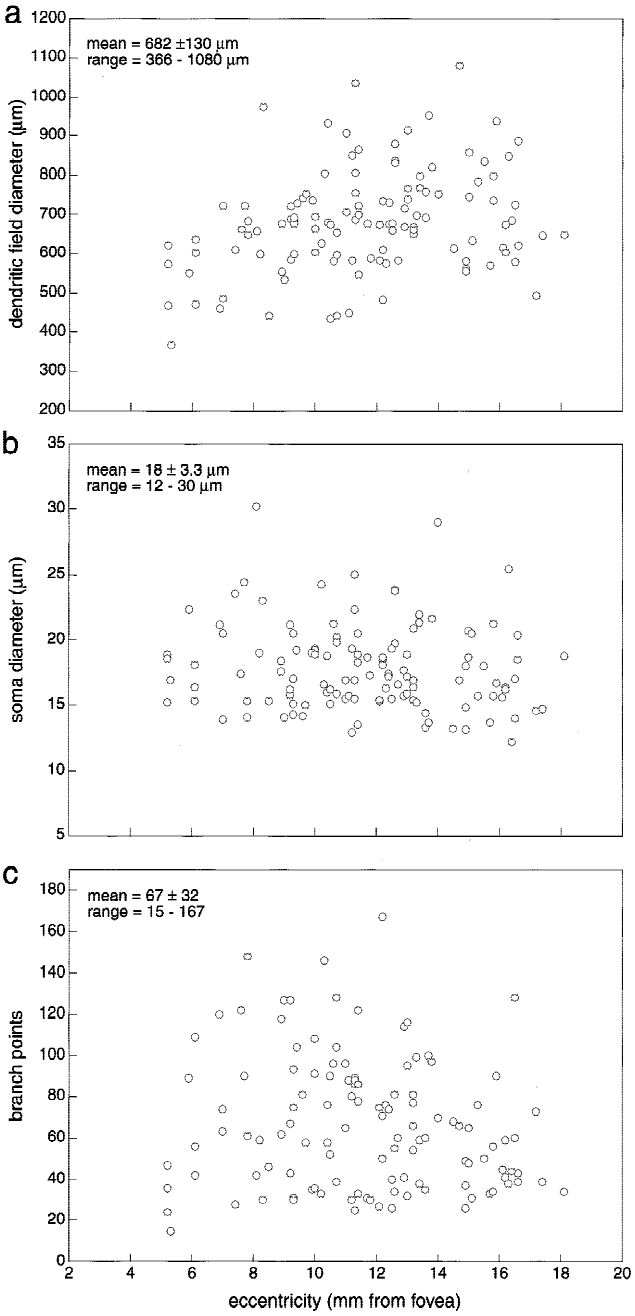

Fig. 3. The wide-field bistratified ganglion cells formed a single cluster when dendritic-field diameter (a) and soma diameter (b) were plotted as a function of eccentricity. The cells showed a broad distribution in the extent of dendritic branching as quantified by the number of terminal branch points (c) although no clustering based on branch point number was apparent.

cells in the present study, however, were unambiguously distinguished from the large sparse monostratified cells on the basis of their clear bistratification. The photomicrograph of Fig. 5a shows another example of a wide-field bistratified cell with a sparse dendritic tree and a simple, radiate pattern of branching.

The remaining 70% of the bistratified cells had thinner dendrites and a more complex, retroflexive, overlapping pattern of branching, as illustrated in the cell tracings of Figs. 4b and 4c.

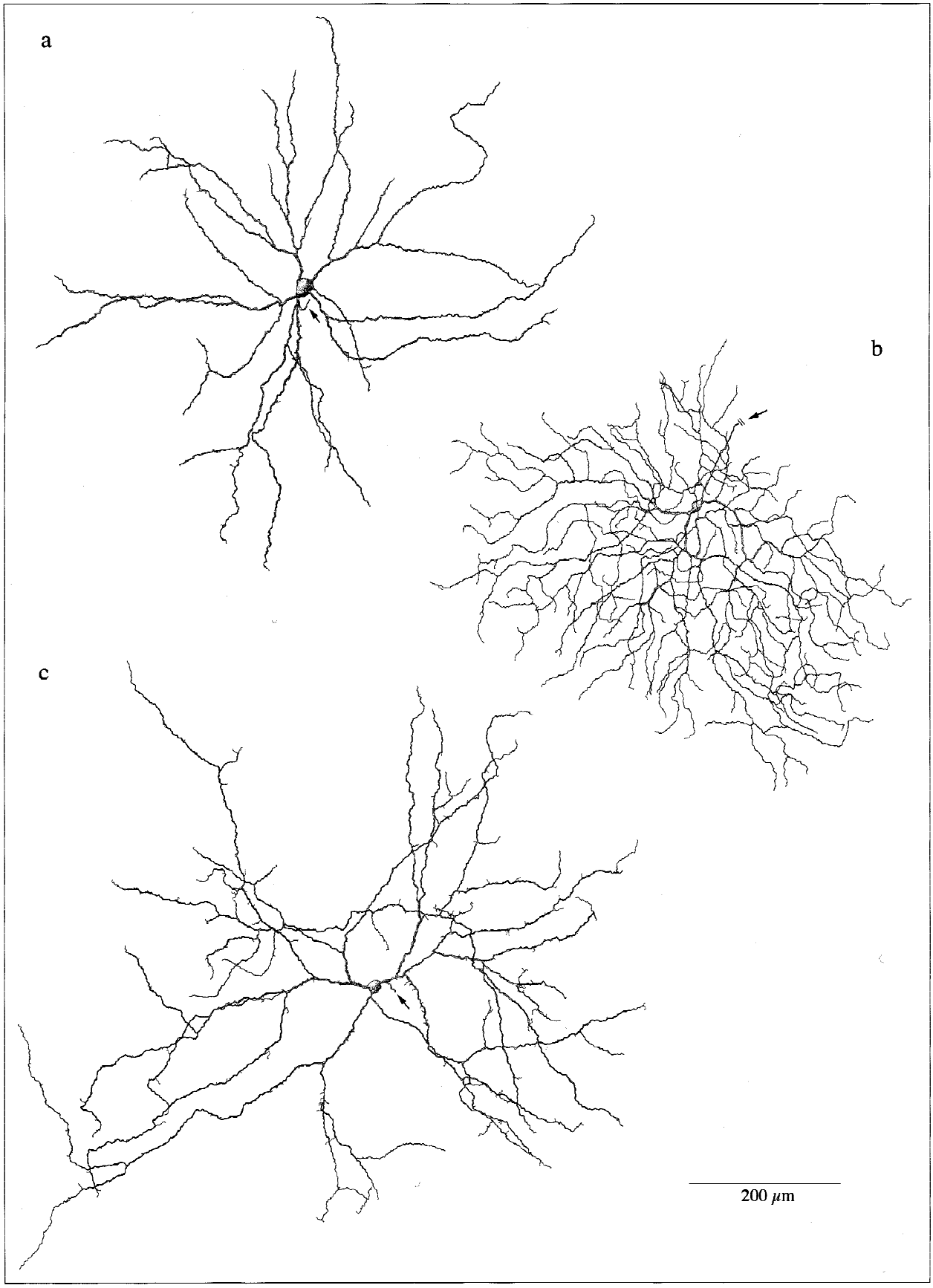

FIGURE 4

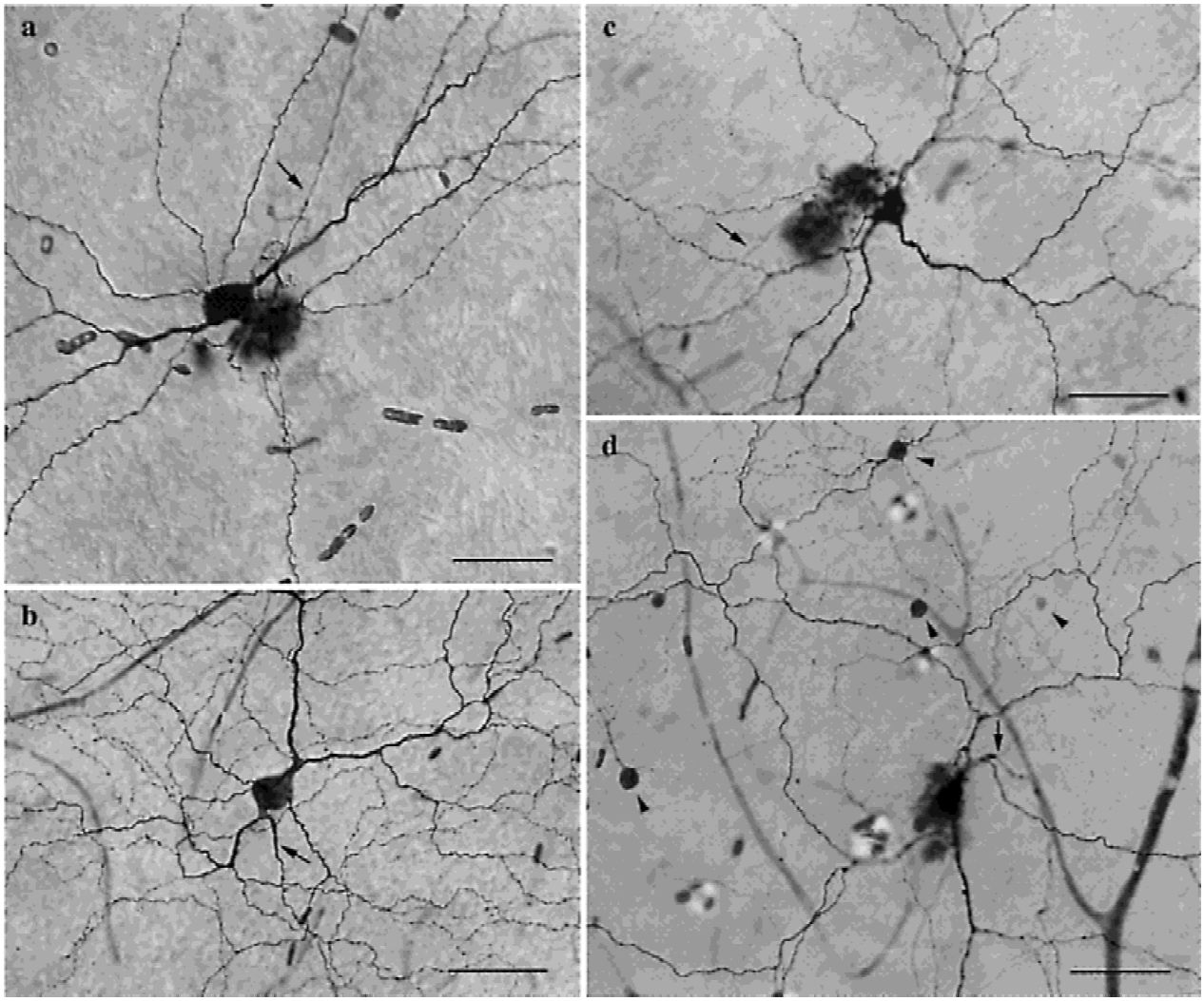

Fig. 5. Photomicrographs of four wide-field bistratified ganglion cells. Arrows indicate axons. Scale bars = 50 μm. (a–c) HRP-filled cells. (a) This cell, located 12.6 mm from the fovea in temporal retina, had thick, slightly spiny dendrites and a simple, radiate pattern of branching similar to the cell shown in Fig. 4a. The sparsely branched (branch points = 34) dendritic tree was 832 μm in diameter and the cell had a soma diameter of 24 μm. Focus is on the inner dendritic arbor. (b) Another example of a very densely branched (branch points = 120) cell similar to the cell of Fig. 4b, located 6.5 mm from the fovea in superior retina. Focus is on the outer dendritic arbor. The cell had a dendritic-field diameter of 460 μm and a soma diameter of 21 μm. (c) Moderately branched (branch points = 75) cell located in inferior retina 9.3 mm from the fovea. Dendritic morphology is similar to the cell of Fig. 4c, with thin, spiny, retroflexive and overlapping dendrites. Dendritic-field diameter was 684 μm; soma diameter was 17 μm. Focus is on the outer dendritic arbor. (d) Neurobiotin-filled cell located 14.7 mm from the fovea in superior retina. Focus is on the outer dendritic arbor. This moderately branched (branch points = 66) cell had a dendritic-field diameter of 1080 μm and a soma 17 μm in diameter, and was similar in dendritic morphology and branching pattern to the cells of Figs. 4c and 5c. The cell showed extensive tracer coupling to a large number of amacrine cells of diverse morphology (arrowheads).

Fig. 4. Camera-lucida tracings of three HRP-filled wide-field bistratified ganglion cells illustrating the morphological diversity of the cells in this group. Axons are indicated by arrows. (a) Sparsely branched (branch points = 28) cell with thick, slightly spiny dendrites and a simple, radiate pattern of branching. The cell had a dendritic-field diameter of 610 μm, a soma diameter of 24 μm, and was located in inferior retina 7.4 mm from the fovea. (b) Densely branched (branch points = 127) cell located in superior retina 9.0 mm from the fovea. The cell had a soma diameter of 14 μm and a dendritic-field diameter of 533 μm, with smooth dendrites and a retroflexive and overlapping pattern of branching. (c) Moderately branched (branch points = 74) cell from superior retina located 12.4 mm from the fovea. The spiny, overlapping dendrites formed a dendritic tree 731 μm in diameter. Soma diameter was 17 μm.

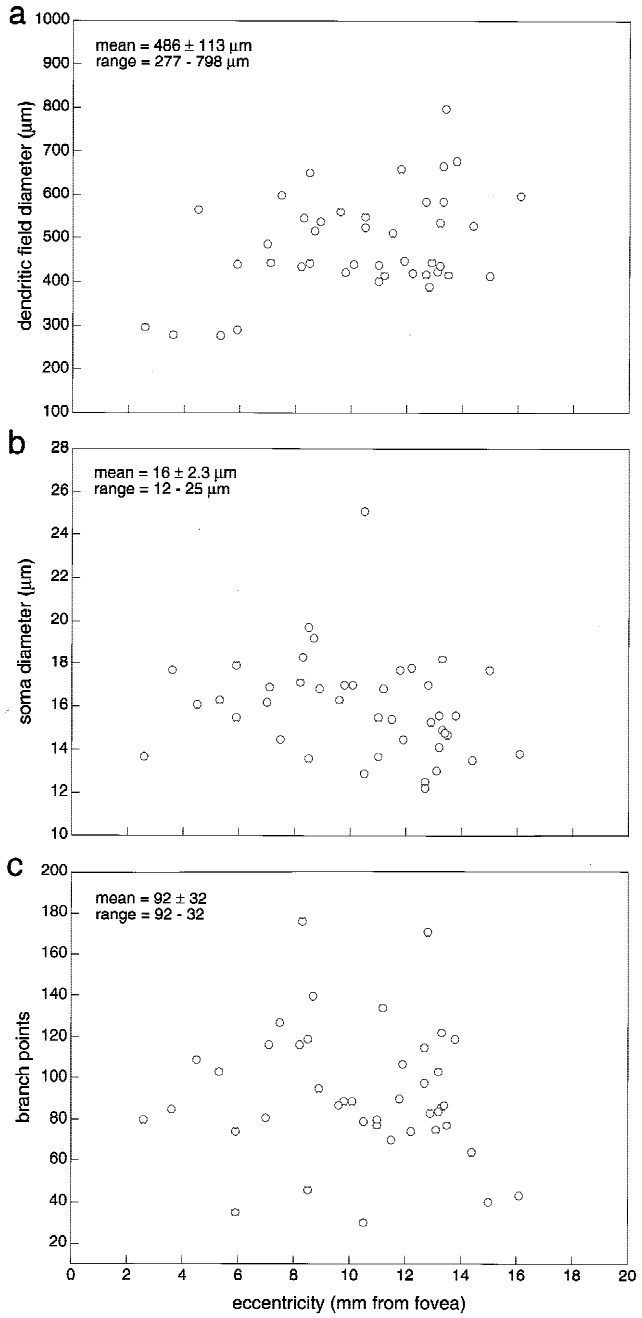

Fig. 6. Wide-field diffuse ganglion cells formed a single cluster when plotted for dendritic-field diameter (a) and soma diameter (b) as a function of eccentricity. Although no clear clustering based on the extent of dendritic branching was apparent (c), the small sample of five cells with fewer than 50 branch points all shared the same morphology as the cell shown in Figs. 7b and 8b.

Most of these cells had spiny dendrites (Fig. 4c) although a few had relatively smooth, nearly spine-free dendrites (Fig. 4b). There was great variability, however, in the extent of dendritic branching among these cells, ranging from very densely branched (Figs. 4b and 5b) to moderately branched (Figs. 4c and 5c), although a few spiny and retroflexively branched cells had dendritic trees as sparsely branched as the cell in Fig. 4a.

There were also differences in the depth of stratification among the wide-field bistratified cells. For example, about ten cells with a morphology similar to the cell shown in Fig. 4a had inner dendrites that appeared more broadly stratified compared to the outer dendrites which were narrowly stratified close to the border of the inner nuclear layer. However, this was also true of two cells with a morphology similar to the cell of Fig. 4c. On the other hand, several cells similar to the cell of Fig. 4a formed inner and outer dendritic arbors that appeared to straddle the middle of the IPL. Due to the degree of vertical shrinkage in our tissue, no attempt was made to precisely quantify this apparent diversity in the level of stratification of the two arbors. These differences, however, do point to the possibility of a larger representation of cell types in our sample than is suggested from the more obvious morphological differences illustrated in Figs. 4 and 5.

Although many of the wide-field bistratified cells had inner and outer dendritic arbors that were coextensive and similar in size, for more than half of the cells this was not the case. The disparity in the size of the inner and outer arbors ranged from cells that were only weakly or partially bistratified—where the majority of the dendritic tree ramified in one portion of the IPL while only a few dendrites, or segments of dendrites, ramified in the other portion—to cells that were strongly bistratified yet had one arbor that was larger or more dense than the other. No relationship between full *versus* partial bistratification and cells exhibiting morphological differences as illustrated in Fig. 4 could be detected. Partial bistratification has been observed in other mammalian retinas and will be discussed in more detail below.

The cell shown in the photomicrograph of Fig. 5d was the only wide-field bistratified cell filled with Neurobiotin, a small molecular-weight tracer that, unlike HRP, can be used to show tracer coupling when cells of the same type (homotypic) or different types (heterotypic) are coupled through gap junctions (Vaney, 1991). The cell in Fig. 5d had a moderately branched, retroflexive dendritic tree similar to the cells shown in Figs. 4c and 5c, and appeared to be heterotypically tracer coupled to a diverse population of amacrine cells (arrowheads in Fig. 5d). All tracer-coupled cells had small somas located in the inner nuclear layer. Although the coupled cells were lightly and incompletely filled, they appeared to comprise possibly three types of amacrine cells: somewhat sparsely branched inner stratifying cells (far left, Fig. 5d), more densely branched outer stratifying cells (topmost cell, Fig. 5d), and smaller cells with only the soma lightly stained (upper right, Fig. 5d). No homotypic tracer coupling or heterotypic coupling to other ganglion cell types was observed.

Diffuse ganglion cells

Forty-two of the wide-field ganglion cells had dendrites that ramified throughout both the inner and outer portions of the IPL. The group was homogeneous in dendritic-field size (Fig. 6a), with a mean dendritic-field diameter (mean ± S.D. = 486 ±113 μm) about 200 μm smaller than the wide-field bistratified cells. Like the wide-field bistratified cells, these cells had medium size somas (mean ± S.D. = 16 ± 2.3 μm) (Fig. 6b). The diffuse cells appeared to be composed of both densely branched and sparsely branched cells that differed in dendritic morphology. The scatter plot of Fig. 6c plots branch point number as a function of eccentricity. Although no clear clustering based on the extent of dendritic branching was observed, the small sample of five cells with fewer than 50 branch points shared the same morphology as the cell shown in

Fig. 7b, while the remaining 37 cells were all similar in dendritic morphology to the cell shown in Fig. 7a.

The dendritic morphology of the majority of diffuse ganglion cells is illustrated by the camera-lucida tracing of the cell in Fig. 7a. The cell had a very densely branched dendritic tree with somewhat thin, very spiny dendrites. These cells were remarkable for the presence of many very fine caliber, twig-like thorny branchlets (inset, Fig. 7a) that both ascended and descended to terminate throughout the IPL. The photomicrograph of Fig. 8a shows another example of these "thorny" diffuse ganglion cells.

A camera-lucida tracing of one of the five sparsely branched diffuse cells is shown in Fig. 7b. The same cell is also shown in the

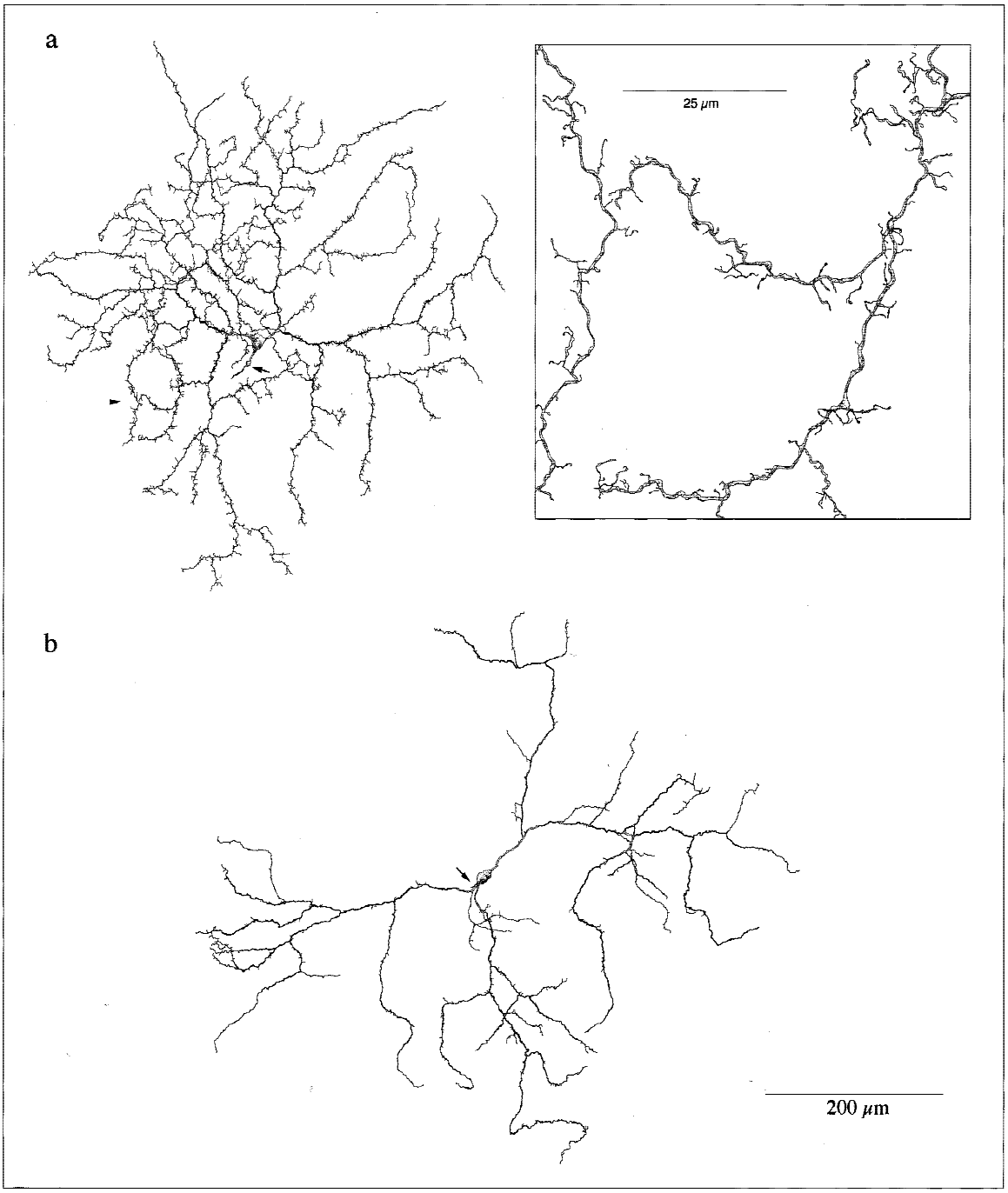

Fig. 7. Camera-lucida tracings of two HRP-filled diffuse wide-field ganglion cells. Axons are indicated by arrows. (a) Located 13.2 mm from the fovea in superior retina, this cell had a densely branched (branch points = 103) dendritic tree with thin, very spiny dendrites. Dendritic-field diameter was 536 μm; soma diameter was 16 μm. The arrowhead indicates a section of the dendritic tree shown in an enlarged view in the inset to illustrate the short, thin, twig-like thorny processes. (b) A sparsely branched diffuse cell from nasal retina 16.1 mm from the fovea. The cell had 43 branch points and a dendritic-field diameter of 597 μm. Soma diameter was 14 μm. This cell is also shown in the photomicrograph of Fig. 8b.

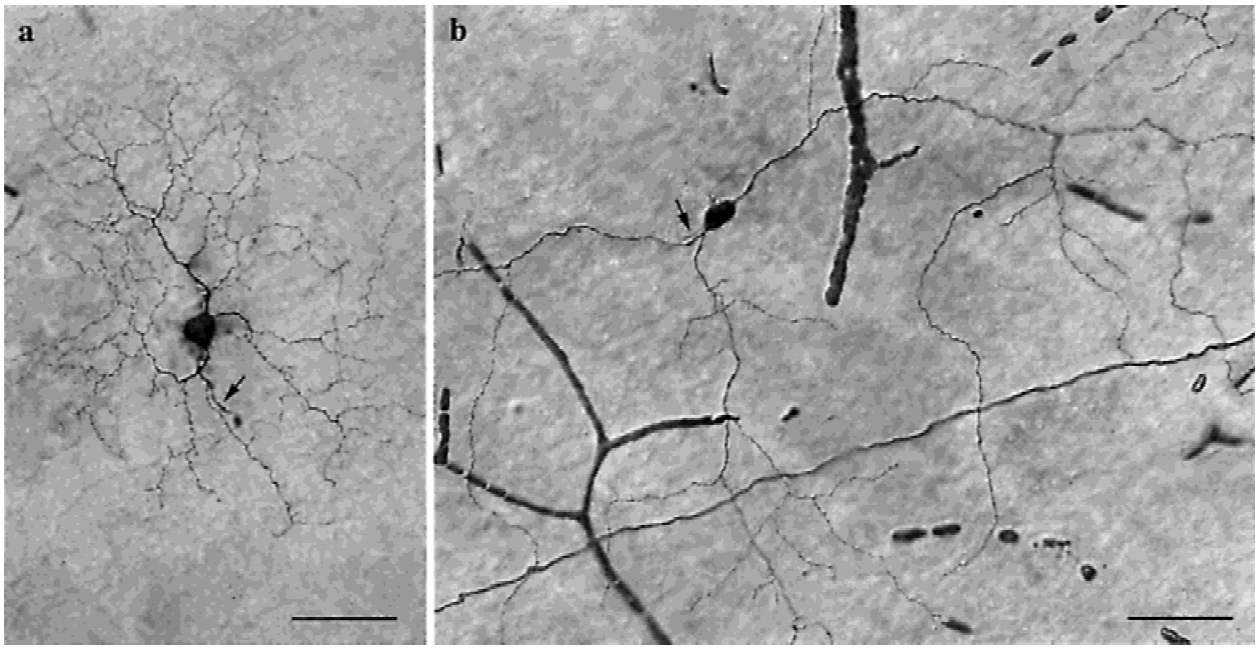

Fig. 8. Photomicrographs of wide-field diffuse ganglion cells. Arrows indicate axons. Scale bars = 50 μm. (a) Another example of a "thorny" diffuse ganglion cell similar to the cell shown in Fig. 7a, located 5.3 mm from the fovea in inferior retina. This more centrally located cell had a dendritic-field diameter of 277 μm and a soma diameter of 16 μm. (b) Same cell as shown in Fig. 7b.

photomicrograph of Fig. 8b. These cells also had thin, spiny dendrites, though the dendrites were not as spiny as the more densely branched cells represented by the tracing of Fig. 7a. The sparsely branched diffuse cells also had very thin, spiny, short terminal processes that ascended and descended throughout the IPL but, again, these were less common than in the densely branched diffuse cells.

Discussion

Classification

Wide-field bistratified cells exhibited a great diversity in the morphology of their dendritic trees, suggesting the presence of multiple cell types, yet without information about their distribution in the ganglion cell layer and the mosaics they form, it is not possible to unequivocally determine the number of discrete types represented by these cells. The cells came from 28 retinas, each of which had only a few or at most a dozen randomly filled cells. We used scatter plots to analyze the cells based on measurable morphological characteristics yet observed no clustering that would indicate subgroups of cells with similar characteristics. We have, therefore, treated the wide-field bistratified cells as one group and have attempted to describe the morphological diversity observed within the group.

The diffuse ganglion cells on the whole were remarkably morphologically homogeneous with the exception of a small group of five cells that had unusually sparsely branched dendritic trees. Although these sparsely branched cells suggest that our sample may contain at least two types of diffuse cells, the small size of the sample of sparsely branched cells made it difficult to observe clear clustering around the parameters used in this study. As with the wide-field bistratified cells, we have, therefore, treated the diffuse cells as one group while noting the differences represented within the group.

Comparisons with other studies

Bistratified ganglion cells

Rodieck and Watanabe (1993) intracellularly injected HRP into monkey retinal ganglion cells labeled with fluorescent tracer following injections into the pretectum, superior colliculus, and parvocellular layers of the lateral geniculate nucleus (LGN). Their results revealed only one type of bistratified cell, the small bistratified cell, projecting to the parvocellular layers of the LGN. However, a great diversity of large bistratified cells were found to project to the superior colliculus. The authors classified these cells into two groups, S- and T-cells, while noting that both groups appeared to contain multiple cell types. Although we were unable to classify the human wide-field bistratified cells into subgroups based on the morphological parameters available to us in this study, about 70% of the cells in our sample had moderate to densely branched dendritic trees with complex and retroflexive patterns of branching very similar to many of the large bistratified cells in Rodieck's and Watanabe's two groups of superior colliculus-projecting cells. For example, the cell of Fig. 4b closely resembles the monkey T-cells, while the cell of Fig. 4c is similar to the monkey S-cells. The monkey S- and T-cells were somewhat smaller than the human bistratified cells, ranging in dendritic-field diameter from ~200 to 600 μm. Differences in dendritic-field size between monkey and human have been observed in several ganglion cell types. Monkey small bistratified cells are smaller than their human counterparts (Dacey, 1993*a*), as are monkey parasol cells (Dacey & Petersen, 1992). The similarities between monkey and human bistratified cells, however, suggest that some of the wide-field bistratified cells in our sample may represent human

correlates of large bistratified cells that project to the superior colliculus in monkey.

Rodieck and Watanabe observed that cells in both of their groups showed a variable degree of bistratification, with some cells very weakly or only partial bistratified, yet the authors reported being unable to find any pattern within this variability. As described above, we also noted the presence of variable degrees of bistratification among the cells in our sample. Partial bistratification has previously been observed in rabbit retina (Amthor et al., 1989*b*). Where a patch of the mosaic formed by a distinct bistratified cell type in rabbit retina has been analyzed, it has been shown that although the distribution of the inner and outer dendritic arbors of individual cells varied in a manner that appeared haphazard when viewed in isolation, the dendrites of the population of neighboring cells together provided a seamless coverage of the retina (Vaney, 1994). It seems reasonable to expect that future similar studies of cell mosaics in primate retina will show that the variability observed in the distribution of the arbors of human and monkey large bistratified cells may be largely due to the variability of individual cells within a distinct cell type, rather than to differences in the pattern and extent of bistratification between cell types.

In a Golgi study of human retina, Kolb et al. (1992) described a bistratified ganglion cell (their G11 cell) that the authors thought may be the human equivalent of the rabbit ON–OFF direction-selective cell type as described by Amthor et al. (1989*a*). In light of subsequent studies in both human and monkey retina (Rodieck & Watanabe, 1993; Dacey, 1993*a*; Dacey & Lee, 1994), it seems more likely that the cell described by Kolb and colleagues was an example of the small bistratified blue-ON cell type. The small size of the dendritic tree and the differences in dendritic morphology between the inner and outer tier dendrites of the Golgi-impregnated cell are characteristic of the small bistratified cell type.

Diffuse ganglion cells

In earlier studies of mammalian retina, several examples of ganglion cells that ramified broadly throughout the IPL were observed in vertical sections of Golgi-impregnated dog (Ramon y Cajal, 1892) and primate (Polyak, 1941) retina. More recent studies of Golgi-impregnated whole-mount human retina (Kolb et al., 1992) described three possible types of diffuse ganglion cells. Of these, only one cell (their cell G5) showed some similarity with the cells in our sample. The cell had a densely branched dendritic tree similar in size and branching pattern to the majority of diffuse cells in the present study, yet the dendrites of the Golgi-impregnated cell were thicker and less spiny and the authors did not observe the presence of the thin, thorny branchlets that were a predominant feature of the HRP-filled cells. Taken together, the results of the Kolb et al. study and the present study suggest that there may be at least four and possibly five types of diffuse ganglion cells in the human retina.

In cat retina, Pu et al. (1994) injected Lucifer yellow and biocytin into ganglion cells retrogradely labeled with fluorescent tracer following injections into the geniculate wing, a thin layer of cells located along the lateral margin of the pulvinar nucleus. With one exception, the labeled cells constituted a single morphological class of monostratified ganglion cells that the authors termed epsilon cells. The exception was one well-filled diffuse ganglion cell with highly branched and overlapping dendrites that exhibited a profusion of fine spines. The cat diffuse ganglion cell bears some similarity with the human cell shown here in Fig. 7a. More recently, O'Brien et al. (1999) reported preliminary results of physiological recordings from two cat diffuse ganglion cells. A detailed morphological characterization of these cells has not yet been published. Although these results from cat retina are intriguing, the evidence is as yet too slim to allow speculation on the possible central projections of diffuse ganglion cells and it would be premature to make definite comparisons between human and cat diffuse cells.

Summary of classes of human ganglion cells

The present study concludes a broader survey of the detailed morphology of human retinal ganglion cells. Ganglion cells in a total of 46 retinas were targeted for intracellular filling with either HRP or Neurobiotin in a random manner, although there was a bias towards cells with medium to large cell bodies. Our total sample of 1241 cells, therefore, while representing much of the diversity of ganglion cells in human retina, would not contain examples of all cell types, especially cells with small somas. Golgi studies of human retina (Kolb et al., 1992) have suggested that there may be as many as 20 different types of ganglion cells. Figs. 9 and 10 summarize the results of our survey and illustrate the morphological diversity of the cells in our sample.

Camera-lucida tracings of monostratified ganglion cells are shown in Fig. 9. The 539 midget ganglion cells made up the largest percentage of all the cells in our sample and included both inner and outer stratifying cell types (Dacey & Petersen, 1992; Dacey, 1993*b*). Parasol cells were the next most common (277 cells) and also included both inner and outer stratifying types (Dacey & Petersen, 1992). Nineteen cells (axon collateral-bearing) had large, sparsely branched dendritic trees and distinctive intraretinal axon collateral processes and represented a single type of inner stratifying cell (Peterson & Dacey, 1998). The 184 wide-field monostratified cells were classified into six groups based on similarities in dendritic-field size and the extent of dendritic branching (Peterson & Dacey, 1999), as illustrated in the tracings of Fig. 9. Of these, three groups (giant very sparse, large very sparse, and large dense) included both inner and outer stratifying cells while the remaining three groups (large sparse, large moderate, and thorny) comprised only inner stratifying cells. In Fig. 10, we have summarized the 119 wide-field bistratified and 42 diffuse ganglion cells of the present study along with a tracing of one of the 61 small bistratified cells described in a previous study (Dacey, 1993*a*). The results of our survey suggest that the human retina contains possibly 20 or more types of ganglion cell types.

These results are in general agreement with the number of cell types reported by Kolb et al. (1992) in their Golgi study of human retina, although the two studies differ in some respects regarding the classification of individual cell types. These differences may be at least partly due to the different methods used. The Golgi method has been widely used to study the morphology of retinal neurons and has contributed greatly to our understanding of the structure of the retina, yet it has the drawback of being unpredictable as to the types, numbers, and distribution of impregnated cells in individual preparations. By using intracellular injection of HRP and Neurobiotin to stain a large sample of ganglion cells at a broad range of eccentricities, we were able to recover the complete morphology of individual cells and control for eccentricity-dependent changes. Our survey adds to our growing understanding of the retina by providing a morphologically detailed and quantitative analysis of the diversity of human retinal ganglion cells.

The structure of human and monkey retina are virtually identical. Old-World monkeys such as the macaque share with humans the property of trichromatic color vision, making monkey retina, and macaque retina especially, ideal models for studying human

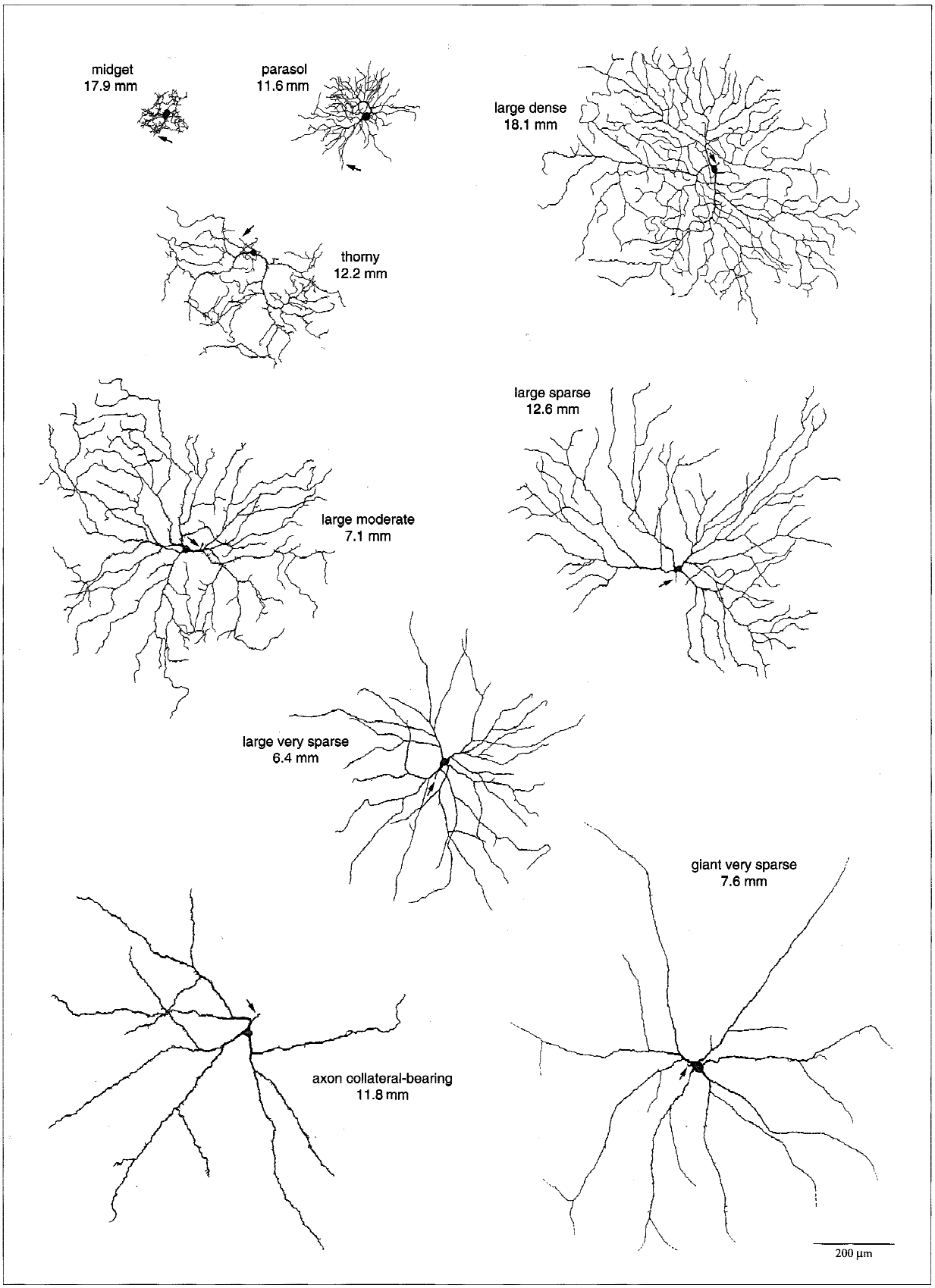

Fig. 9. Camera-lucida tracings summarizing the diversity of human monostratified ganglion cells revealed through intracellular injection of HRP. Axons are indicated by arrows. Numbers next to cells are distances from the fovea. From Peterson and Dacey, 1999.

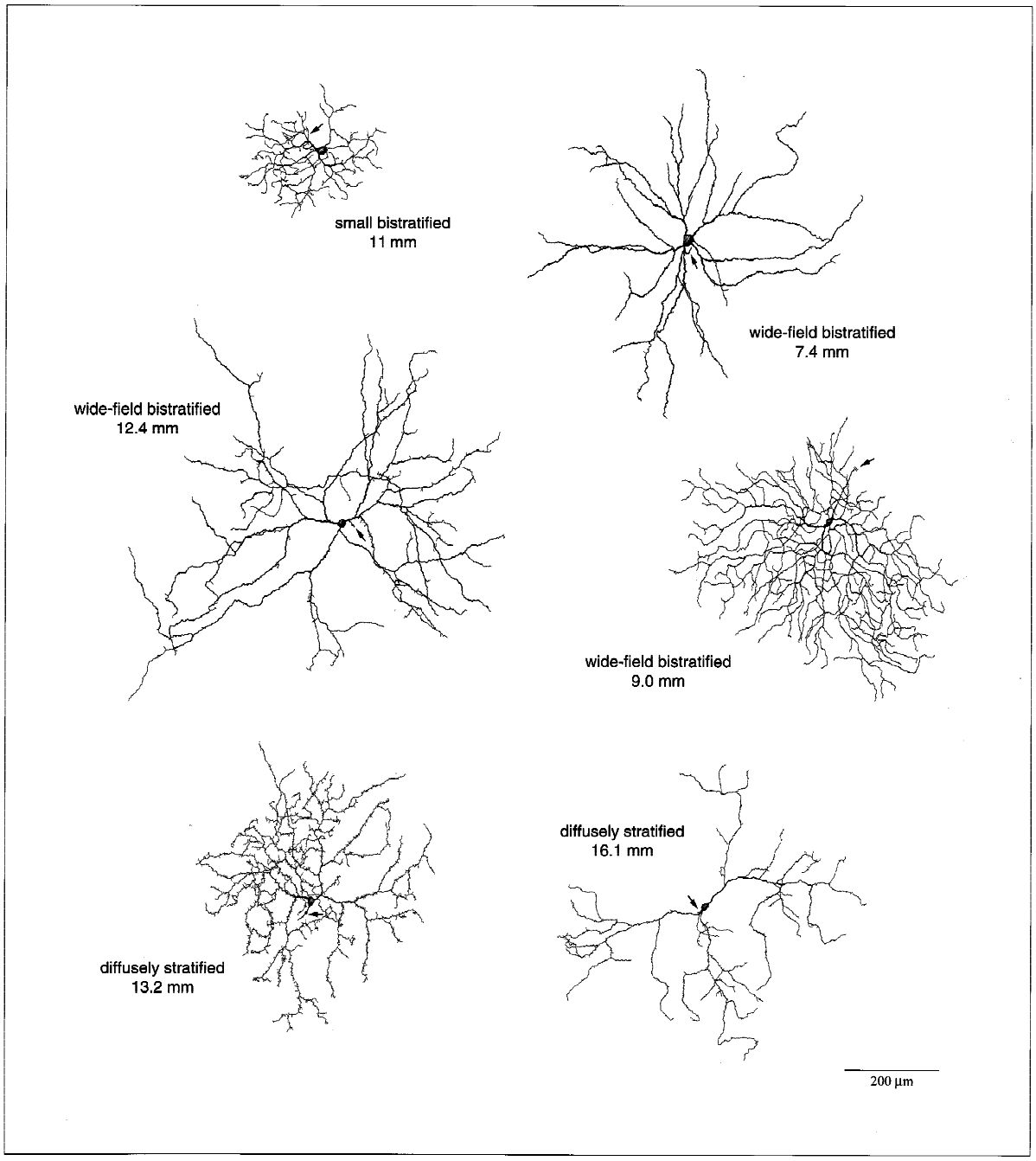

Fig. 10. Camera-lucida tracings summarizing the diversity of human bistratified and diffuse ganglion cells revealed through intracellular injection of HRP. Arrows indicate axons. Numbers next to cells are distances from the fovea. Three examples of the diversity within the group of wide-field bistratified cells, and two examples of the diversity within the group of diffuse cells are illustrated. These cells are also shown in Figs. 4 and 7. The small bistratified cell is from Dacey, 1993*a*.

retinal structure and function. To date, the morphology, physiology, and central projections of parasol, midget, and small bistratified ganglion cells in monkey retina have been well studied (Boycott & Dowling, 1969; Leventhal et al., 1981, 1993; Perry & Cowey, 1984; Watanabe & Rodieck, 1989; Dacey & Petersen, 1992; Rodieck & Watanabe, 1993; Dacey, 1993*a*, 2000; Dacey & Lee, 1994; Silveira et al., 1994; Ghosh et al., 1996; Yamada et al., 1996). Although these three cell classes make up the majority of ganglion cells and are important for visual processing, it is clear that they represent only a small fraction of the number of ganglion cell types. A full understanding of the diverse population of human wide-field monostratified, bistratified, and diffuse ganglion cells awaits future studies in primate retina where, combining intracellular staining and recording along with retrograde labeling from central targets, it will be possible to fully characterize the distinct cell types represented by these cell classes.

Acknowledgments

Special thanks to Kim Allen of the Lions Eye Bank, and to Toni Haun and Keith Boro for technical help. This work was supported by NIH Grant EY06678.

References

Amthor, F.R., Oyster, C.W. & Takahashi, E.S. (1984). Morphology of ON–OFF direction-selective ganglion cells in the rabbit retina. *Brain Research* **298**, 187–190.

Amthor, F.R., Takahashi, E.S. & Oyster, C.W. (1989*a*). Morphologies of rabbit retinal ganglion cells with complex receptive fields. *Journal of Comparative Neurology* **280**, 97–121.

Amthor, F.R., Takahashi, E.S. & Oyster, C.W. (1989*b*). Morphologies of rabbit retinal ganglion cells with concentric receptive fields. *Journal of Comparative Neurology* **280**, 72–96.

Barlow, H.B., Hill, R.M. & Levick, W.R. (1964). Retinal ganglion cells responding selectively to direction and speed of image motion in the rabbit. *Journal of Physiology* (London) **173**, 377–407.

Boycott, B.B. & Dowling, J.E. (1969). Organization of the primate retina: Light microscopy. *Philosophical Transactions of the Royal Society B* (London) **255**, 109–184.

Dacey, D.M. (1993*a*). Morphology of a small-field bistratified ganglion cell type in the macaque and human retina. *Visual Neuroscience* **10**, 1081–1098.

Dacey, D.M. (1993*b*). The mosaic of midget ganglion cells in the human retina. *Journal of Neuroscience* **13**, 5334–5355.

Dacey, D.M. (2000). Parallel pathways for spectral coding in primate retina. In *Annual Review of Neuroscience,* ed. Cowan, W.M., Shooter, E.M., Stevens, C.F. & Thompson, R.F., pp. 743–775. Palo Alto, California: Annuals Reviews.

Dacey, D.M. & Lee, B.B. (1994). The 'blue-on' opponent pathway in primate retina originates from a distinct bistratified ganglion cell type. *Nature* **367**, 731–735.

Dacey, D.M. & Petersen, M.R. (1992). Dendritic field size and morphology of midget and parasol ganglion cells of the human retina. *Proceedings of the National Academy of Sciences of the U.S.A.* **89**, 9666–9670.

Dacey, D.M., Petersen, M.R. & Allen, K.A. (1991). Beyond the midget and parasol cells of the human retina. *Investigative Ophthalmology and Visual Science* (Suppl.) **32**, 1130

Famiglietti, E.V. (1992). Dendritic co-stratification of ON and ON–OFF directionally selective ganglion cells with starburst amacrine cells in rabbit retina. *Journal of Comparative Neurology* **324**, 322–335.

Ghosh, K.K., Goodchild, A.K., Sefton, A.E. & Martin, P.R. (1996). Morphology of retinal ganglion cells in a New World monkey, the marmoset *Callithrix jacchus*. *Journal of Comparative Neurology* **366**, 76–92.

Kolb, H., Linberg, K.A. & Fisher, S. (1992). Neurons of the human retina: A Golgi study. *Journal of Comparative Neurology* **318**, 147–187.

Leventhal, A.G., Keens, J. & Törk, I. (1980). The afferent ganglion cells and cortical projections of the retinal recipient zone (RRZ) of the cat's 'pulvinar complex.' *Journal of Comparative Neurology* **194**, 535–554.

Leventhal, A.G., Rodieck, R.W. & Dreher, B. (1981). Retinal ganglion cell classes in the Old World monkey: Morphology and central projections. *Science* **213**, 1139–1142.

Leventhal, A.G., Thompson, K.G. & Liu, D. (1993). Retinal ganglion cells within the foveola of New World (*Saimiri sciureus*) and Old World (*Macaca fascicularis*) monkeys. *Journal of Comparative Neurology* **338**, 242–254.

O'Brien, B.J., Isayama, T. & Berson, D.M. (1999). Light responses of morphologically identified cat ganglion cells. *Investigative Ophthalmology and Visual Science* **40**, S815

Oyster, C.W. & Barlow, H.B. (1967). Direction-selective units in rabbit retina: Distribution of preferred directions. *Science* **155**, 841–842.

Oyster, C.W., Amthor, F.R. & Takahashi, E.S. (1993). Dendritic architecture of ON–OFF direction-selective ganglion cells in the rabbit retina. *Vision Research* **33**, 579–608.

Perry, V.H. & Cowey, A. (1984). Retinal ganglion cells that project to the superior colliculus and pretectum in the macaque monkey. *Neuroscience* **12**, 1125–1137.

Peterson, B.B. & Dacey, D.M. (1998). Morphology of human retinal ganglion cells with intraretinal axon collaterals. *Visual Neuroscience* **15**, 377–387.

Peterson, B.B. & Dacey, D.M. (1999). Morphology of wide-field, monostratified ganglion cells of the human retina. *Visual Neuroscience* **16**, 107–120.

Polyak, S.L. (1941). *The Retina*. Chicago, Illinois: University of Chicago Press.

Pu, M., Berson, D. M. & Pan, T. (1994). Structure and function of retinal ganglion cells innervating the cat's geniculate wing: An *in vitro* study. *Journal of Neuroscience* **14**, 4338–4358.

Ramon y Cajal, S. (1892). La rètine des vertèbrès. *La Cellule* **9**, 119–257. Translated into English by D. McGuire and R.W. Rodieck. In *The Vertebrate Retina: Principles of Structure and Function*. San Francisco, California: W. H. Freeman, 1973.

Rodieck, R.W. & Watanabe, M. (1993). Survey of the morphology of macaque retinal ganglion cells that project to the pretectum, superior colliculus, and parvicellular laminae of the lateral geniculate nucleus. *Journal of Comparative Neurology* **338**, 289–303.

Silveira, L.C.L., Yamada, E.S., Perry, V.H. & Picanco-Diniz, C.W. (1994). M and P retinal ganglion cells of diurnal and nocturnal New-World monkeys. *NeuroReport* **5**, 2077–2081.

Vaney, D.I. (1991). Many diverse types of retinal neurons show tracer coupling when injected with biocytin or Neurobiotin. *Neuroscience Letters* **125**, 187–190.

Vaney, D.I. (1994). Territorial organization of direction-selective ganglion cells in rabbit retina. *Journal of Neuroscience* **14**, 6301–6316.

Watanabe, M. & Rodieck, R.W. (1989). Parasol and midget ganglion cells of the primate retina. *Journal of Comparative Neurology* **289**, 434–454.

Yamada, E.S., Silveira, L.C.L. & Perry, V.H. (1996). Morphology, dendritic-field size, somal size, density, and coverage of M and P ganglion cells of dichromatic *Cebus* monkeys. *Visual Neuroscience* **13**, 1011–1029.

Yang, G. & Masland, R.H. (1992). Direct visualization of the dendritic and receptive fields of directionally selective retinal ganglion cells. *Science* **258**, 1949–1952.